REPORT OF INVESTIGATIONS/1988

Dielectric Properties of Low-Loss Minerals

By R. H. Church, W. E. Webb, and J. B. Salsman

BUREAU OF MINES

UNITED STATES DEPARTMENT OF THE INTERIOR

Report of Investigations 9194

Dielectric Properties of Low-Loss Minerals

By R. H. Church, W. E. Webb, and J. B. Salsman

UNITED STATES DEPARTMENT OF THE INTERIOR
Donald Paul Hodel, Secretary

BUREAU OF MINES
T S Ary, Director

This report is based upon work done under an agreement between the University of Alabama and the Bureau of Mines.

Library of Congress Cataloging in Publication Data:

Church, Ronald H.

Dielectric properties of low-loss minerals.

(Bureau of Mines Report of investigations; 9194)

Bibliography: p. 14

1. Mineralogy–Electric properties. 2. Mineralogy–Thermal properties. I. Webb, William E. II. Salsman, J. B. III. Title. IV. Series: Report of investigations (United States. Bureau of Mines); 9194.

TN23.U43 [QE364] 622 s [549'.127] 88-600145

CONTENTS

ILLUSTRATIONS

TABLES

UNIT OF MEASURE ABBREVIATIONS USED IN THIS REPORT

$Cal \cdot g^{-1} \cdot °C^{-1}$	calorie per gram per degree celsius	MΩ/Cm	megohm per centimeter
$Cal \cdot s^{-1} \cdot cm^{-3}$	calorie per second per cubic centimeter	min	minute
cm	centimeter	Ω	ohm
cm/s	centimeter per second	pct	percent
°C	degree Celsius	rad/s	radian per second
°F	degree farenheit	s	second
F/cm	farad per centimeter	S	siemens
GHz	gigahertz	V	volt
$g \cdot cm^{-3}$	gram per cubic centimeter	V/cm	volt per centimeter
Hz	hertz	Vol pct	volume percent
kW	kilowatt	W/cm^2	watt per square centimeter
MHz	megahertz		

DIELECTRIC PROPERTIES OF LOW-LOSS MINERALS

By R. H. Church,[1] W. E. Webb,[2] and J. B. Salsman[3]

ABSTRACT

As part of the research effort on investigating the effects of microwave energy upon the chemical and physical properties of different minerals and ores, the Bureau of Mines has conducted basic research into identifying those properties of minerals that are affected by microwave energy, namely, the dielectric constant and loss tangent. These properties were determined utilizing the theory of microwave propagation in a coaxial waveguide filled with a dielectric material and measuring the input impedance with an RF impedance analyzer that operates from 1 MHz to 1 GHz. By knowing the microwave frequency and filling the waveguide with a powdered mineral, the dielectric properties of the mineral sample were determined. From these dielectric properties, theoretical microwave heating characteristics of each mineral could be calculated. These same mineral samples were then irradiated by a 915 MHz 30 kW variable power microwave oven and dielectric heating studies were performed. A comparison of the theoretical heating characteristics and the results from actual dielectric heating studies was conducted to evaluate the dielectric property measurements on each mineral.

This report presents the results of the Bureau's research in identifying the dielectric properties of low-loss minerals according to the mineralogical classification scheme along with their irradiation studies. Though far from complete, this study represents some of the more frequently encountered low-loss minerals.

[1]Mining engineer.
[2]Physical scientist.
[3]Electrical engineer.
Tuscaloosa Research Center, Bureau of Mines, Tuscaloosa, AL.

INTRODUCTION

The Bureau of Mines conducted research to determine if microwave heating can influence the response of a particular process to enhance mineral beneficiation. In order to predict the rate at which a mineral will heat in an electromagnetic field (microwave), it is necessary to know both its thermal and electrical properties. In particular, it is necessary to know the dielectric constant (ϵ_r), also known as the relative permittivity, and loss tangent ($\tan\delta$) of the mineral since the rate that microwave power is absorbed is proportional to the product of these two quantities.

Much work has previously been devoted to determine the thermal properties of minerals (*1-2*).[4] However, data available in literature on permittivities and loss tangents of important minerals are either inadequate or nonexistent.

Only a few references give any data on the dielectric properties of minerals, and those are limited. Furthermore, much of the published data omits the frequency range from 30 MHz to 3 GHz (*3-6*). Until the recent development of advanced electronic circuitry this has been a difficult frequency range in which to work; being too high for conventional radio frequency (RF) techniques and too low for microwave techniques. It is this frequency range that is of interest however, as it includes the 915 MHz and 2.45 GHz frequency bands allocated for use in industrial, scientific, and medical (ISM) applications. It is the range in which the dielectric heating experiments were conducted.

Another problem associated with using published data is that minerals are not pure compounds, but are usually mixtures whose composition can vary. The molecular composition of most minerals varies significantly. Some minerals are composed of various mixtures of different molecules each of which can and often do form different elemental compositions for the same mineral. Biotite, $H_2K(Mg,Fe)_3Al(SiO_4)_3$, a type of mica, is a good example of different elemental composition. Essentially, the composition can vary from 0 to 17 pct Mg and 0 to 33 pct Fe (*7*). This difference in magnesium and iron can affect the dielectric properties significantly. Mineral samples taken from different deposits, or even from different parts of the same deposit, could have different electrical properties. The mineral coal (*7*) has been subdivided into different classes (anthracite, bituminous, subbituminous, etc.) and, even in the same class, significantly different dielectric properties exist for the same deposit (*8*), often varying by 50 pct. Other factors, such as water content, can also affect both the dielectric constant and loss tangent. Thus, even when published data exist it is not clear that they can be indiscriminately applied to the particular sample under investigation, unless all parameters have been identified.

OTHER AREAS OF INTEREST

Other areas of interest in which the scientific community could benefit from an increased knowledge of the dielectric properties of minerals include application to through-the-earth communications, ground penetrating radar (GPR), and dielectric separation of minerals.

Efforts to produce electromagnetic systems for the location of trapped miners and to communicate with them require a knowledge of the dielectric properties of the transmission medium, namely the geologic strata through which the electromagnetic waves will propagate. The attenuation of electromagnetic signals through the Earth's crust is related to the dielectric properties of the minerals composing the individual rock types (*9*).

The Bureau has conducted extensive research in this area including on-site cataloging of the attenuation characteristics of overlying mine strata (*10*). An extensive knowledge of the dielectric properties would aid in developing propagation models and improving the performance of through-the-earth electromagnetic communication systems.

In recent years, GPR systems have been used in a number of applications in the mining industry, including geological exploration (*11*), measurement of coal seam thickness (*12*), location of abandoned mine tunnels, voids and seam anomalies (*13-14*), and in identifying mine roof structures in underground coal mines that could lead to roof failure (*15*). The design criteria for a GPR system are a combination of frequency, depth of penetration, and power requirements. Each of these in turn is dependent upon the dielectric properties of the strata through which the system will operate. Knowing the dielectric properties at the desired frequency would aid in optimizing the system design.

Another application is dielectric separation of minerals (*16*). The Bureau has designed and constructed a dielectric separator, which generates a high-gradient, alternating electric field within a dielectric fluid medium. Mineral particles with dielectric constant higher than the dielectric constant of the fluid move in the direction of the highest field gradient. Then, by using a dielectric fluid somewhere between the dielectric constant of the desired mineral and the associated gangue, a separation can be made.

[4]Italic numbers in parentheses refer to items in the list of references preceding the appendixes at the end of this report.

MEASUREMENT OF DIELECTRIC PROPERTIES OF MINERALS

The dielectric properties of several low-loss minerals were measured by a technique developed by the Bureau. This technique involves electromagnetic theory and Maxwell's equations of microwave propagation where ϵ_r, the conductivity, σ,and thus, tanδ of each mineral can be measured indirectly through an RF impedance analyzer. The following sections will discuss the instrumentation that was used, the theory involved, along with a discussion of the accuracy and limitations. The dielectric properties of each mineral as measured by this technique are also included in tabular form. These same properties are again given in graphic form in appendix A in order that possible trends of the dielectric properties as a function of frequency may be recognized.

INSTRUMENTATION

The ϵ_r and tanδ of a mineral are measured in a short section of rigid coaxial waveguide. The waveguide is filled with a mixture of the powdered mineral and a liquid of known dielectric properties. The waveguide is filled to the end with the liquid first. The mineral is then gradually poured into the waveguide and compacted to assure that no gaps in the mineral along the length of the waveguide are formed. The mineral is continually poured and compacted in the waveguide until it also fills the waveguide to the end. The open end of the waveguide is then capped with a solid brass screw-on cap, which not only seals the waveguide, but also acts as a short at the end of the waveguide. The waveguide is then connected to an RF impedance analyzer (fig. 1), which measures the reflection coefficient at its input in the frequency range of 300 MHz to 1 GHz in 100 MHz intervals. The impedance at the input of the waveguide is computed at each frequency by a microprocessor in the impedance analyzer. The effective ϵ_r and tanδ of the mineral-liquid mixture can then be calculated. By using a series of liquids with different dielectric properties, it is possible to determine the dielectric properties of the mineral.

THEORY

Through Maxwell's equations of wave propagation, it can be shown that the input impedance, Z_{in}, of a transmission line of length, ℓ, with a characteristic impedance, Z_o, is related to the reflection coefficient, Γ, by (*17*)

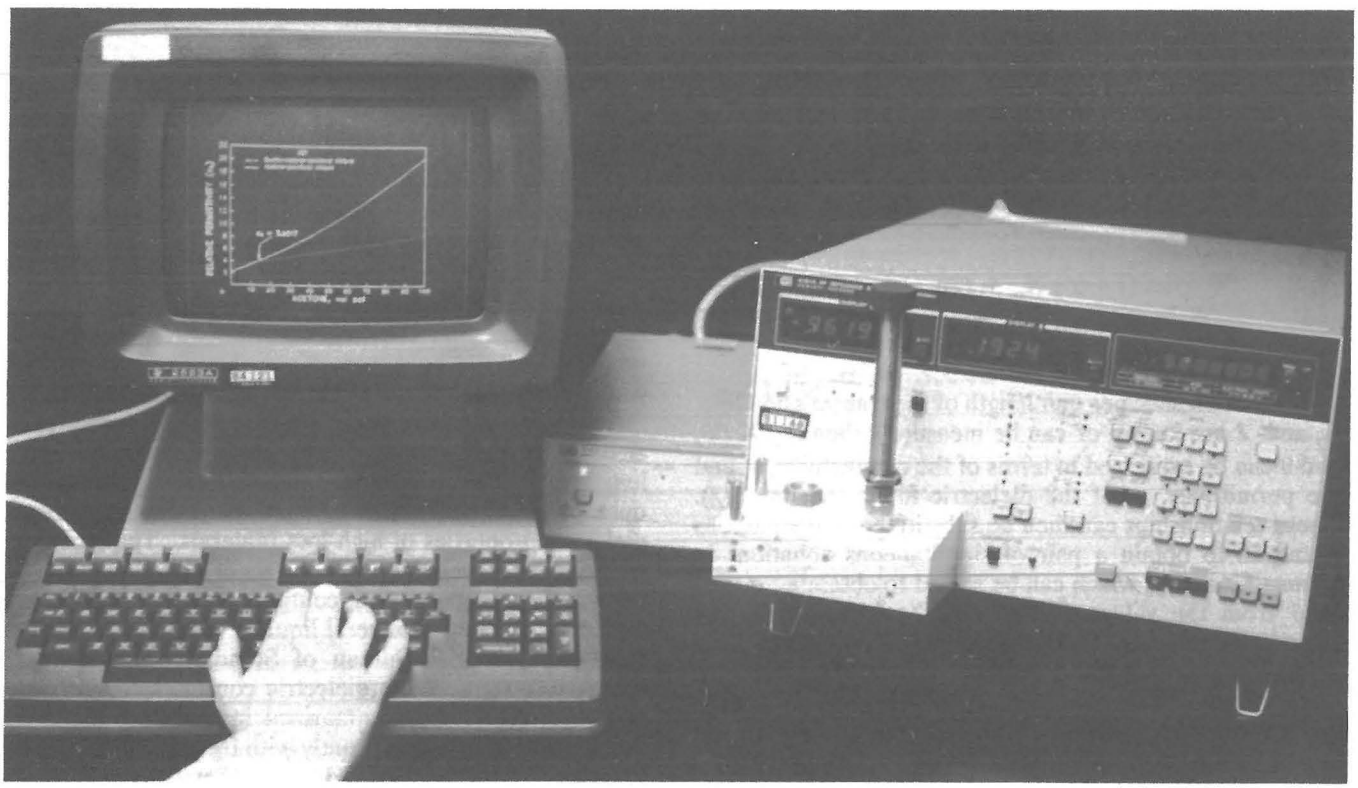

Figure 1. - Dielectric property measurement equipment including impedance analyzer, coaxial line, and computer.

$$\Gamma = \frac{Z_{in} - Z_o}{Z_{in} + Z_o} \quad (1)$$

or $$Z_{in} = \frac{1 + \Gamma}{1 - \Gamma} Z_o. \quad (2)$$

The load reflection coefficient, Γ_{load}, is related to Γ by

$$\Gamma = \Gamma_{load} e^{-2\gamma\ell} \quad (3)$$

where $$\gamma = \alpha + j\beta \quad (4)$$

is the complex propagation constant for the line with α the attenuation constant and β the phase constant. For an ideal short circuit at the end of the line, $\Gamma_{load} = -1$. Equation 2 becomes,

$$Z_{in} = \frac{1 - e^{-2\gamma\ell}}{1 + e^{-2\gamma\ell}} Zo. \quad (5)$$

since $$Z_{in} = R_{in} + jX_{in} \quad (6)$$

and $$Z_o = R_o + jX_o \quad (7)$$

and letting $$u = e^{-2\alpha\ell} \quad (8)$$

equation 5 may be separated into its real and imaginary parts leaving,

$$R_{in} = \frac{(1 - u^2) R_o - (2u \cdot \sin 2\beta\ell) X_o}{1 + u^2 + (2u \cos 2\beta\ell)} \quad (9)$$

and $$X_{in} = \frac{(1 - u^2) X_o + (2u \cdot \sin 2\beta\ell) R_o}{1 + u^2 + (2u \cos 2\beta\ell)} \quad (10)$$

If the resistance per unit length of the transmission line, R, and ℓ are known or can be measured, then R_o, X_o, β, and u can be expressed in terms of the conductivity, σ, and the permittivity, ϵ, of the dielectric filling the line (*17*). These relationships can then be substituted into equations 9 and 10 to obtain a pair of simultaneous equations in terms of σ and ϵ, which can be solved to obtain ϵ_r, σ, and tanδ from the values of R_{in} and X_{in} measured by the impedance analyzer. For a more detailed analysis of these equations see reference 18.

DETERMINATION OF DIELECTRIC PROPERTIES OF BULK MATERIAL

The values of σ and ϵ that are determined as described above, are not the values of σ and ϵ of the mineral in question, but are the dielectric properties of the mineral-liquid mixture. The procedure must be repeated a series of times using different liquid mixtures in order that a relationship between the mineral and liquid dielectric properties can be determined.

To ensure a continuously varying ϵ_r of the liquid, mixtures of two liquids were used, one liquid being of lower ϵ_r than the other. The liquids were mixed by varying the percent volume of each in increments of 10 pct. For minerals with ϵ_r's in the range of 2.3 to 20.7, mixtures of perchloral (tetrachloroethylene) and acetone were used. For minerals with ϵ_r in the range of 20.7 to 78, acetone and deionized water mixtures were used. The ϵ_r's of the mixtures were measured and, not surprisingly, found to be an almost linear function of the percentage of the higher dielectric liquid. The best fit for the data was a quadratic curve using the least mean square technique (figs. 2-3).

The ϵ_r's of the liquid mixtures along with the powdered mineral were measured next. These data were also fit to a quadratic curve. The two equations of the curves, one of the liquid mixtures alone and the other of the liquid mixtures with the powdered mineral, were then set equal to each other and solved. The resulting solution is the ϵ_r(or σ) of the bulk mineral (figs. 4-5). From σ, tanδ, can be determined using the relationship

$$\tan\delta = \frac{\sigma}{\epsilon,} \quad (11)$$

where is the angular frequency and ϵ is the permittivity of the mineral.

ACCURACY AND LIMITATIONS

According to the manufacturer's specifications, the impedance analyzer used in the measurement procedure is accurate within 1 pct. Some approximations have been used in deriving this technique and for the frequency range of interest, (300-1,000 MHz), these approximations hold true (*18*). When measuring minerals with high conductivities, such as metallic sulfides and some coals, the approximation that the losses in the waveguide can be neglected did not hold true. Since the waveguide is filled with the mineral and the mineral is nearly as conductive as the walls of the waveguide; the mineral creates a short circuit, therefore the wave does not propagate the entire length of the line. Presently another technique, using an open-ended coaxial line, is being employed to measure the dielectric properties of high-loss minerals. The technique of filling a waveguide with a material to measure its dielectric properties was confirmed by measuring the dielectric constant of several liquids, which were obtained from the National Bureau of Standards (NBS). The measured values of the dielectric constants compared to the NBS values are summarized in table 1. Since the conductivity varies significantly with frequency, there were no values from NBS for conductivity that were valid for the frequency ranges measured by the impedance analyzer. But, because these liquids are low-loss materials, the dielectric constant is relatively constant throughout the frequency range of interest.

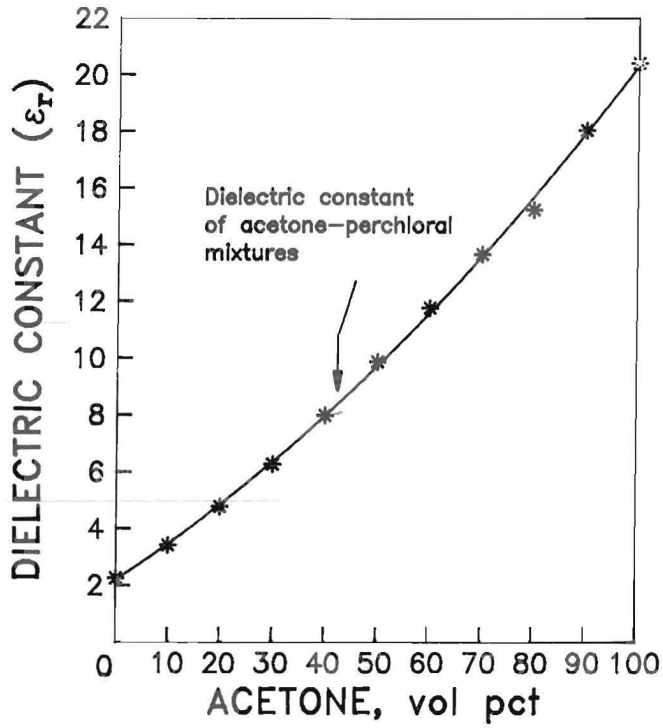

Figure 2. - Dielectric constant versus volume percentage of acetone for acetone-perchloral mixtures.

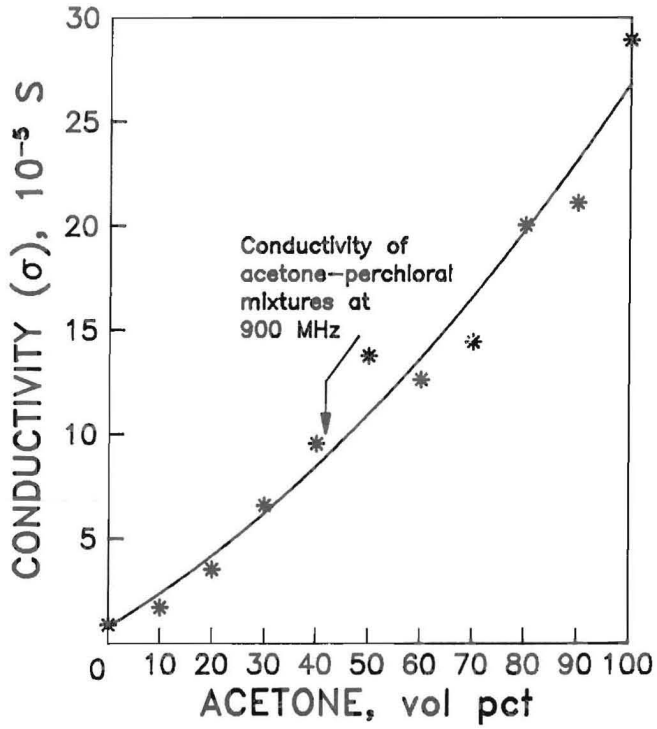

Figure 3. - Conductivity versus volume percentage of acetone for acetone-perchloral mixtures measured at 900 MHz.

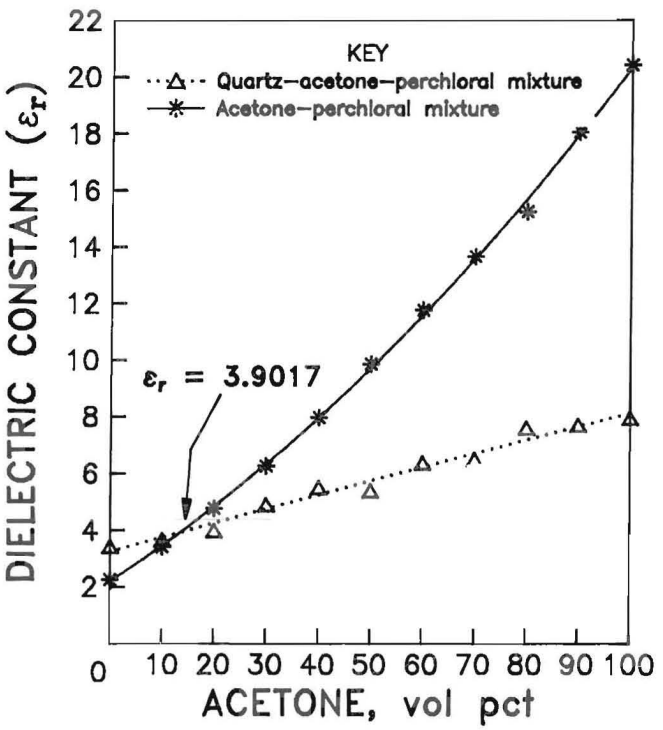

Figure 4. - Dielectric constant of quartz.

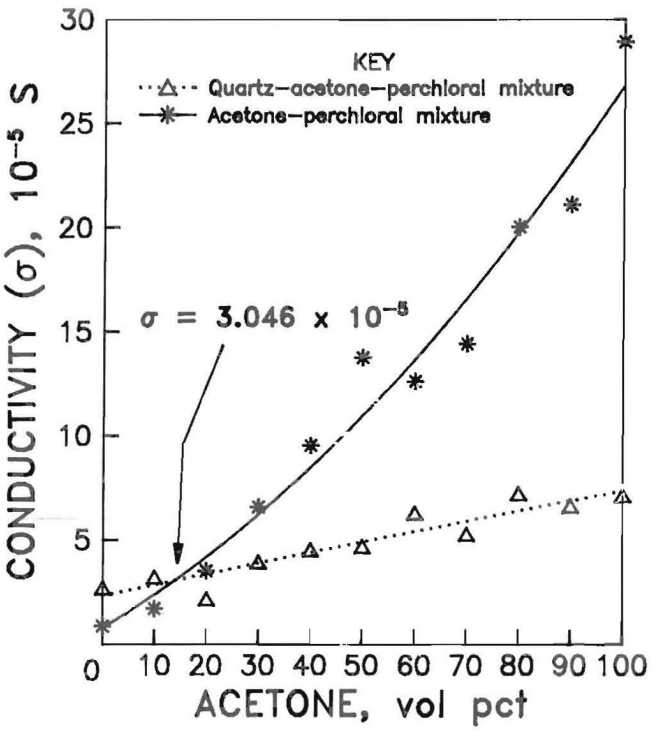

Figure 5. - Conductivity of quartz.

TABLE 1. - Comparison of measured dielectric constants with published data for liquids

Liquid	Dielectric constant (ϵ_r)[1]				Difference, pct
	Measured		Reference data		
	Average value	Number of measurements	Value	Reference source	
Dielectric constant reference material:					
Cyclohexane	1.953	3	[1]2.01517	NBS	3.10
1,2-dichloroethane	10.14	3	10.3551	NBS	2.07
Nitrobenzene	33.72	3	34.7416	NBS	2.94
Reagent-grade material:					
Perchloral	2.27	2	2.30	Von Hipple (5)	1.30
Acetone	20.53	2	20.70	Von Hipple	.80
Deionized water at 18 MΩ/cm	75.63	2	78.54	Von Hipple	3.70

NBS National Bureau of Standards.

[1]All liquids were measured and reference data obtained at 25° C.

Published values of the dielectric constant of a few minerals were found in Young (*4*). These values compared to the values obtained when measuring the dielectric properties of the same minerals by this technique are summarized in table 2.

Validity of the measured values of ϵ_r on the NBS liquids was within ±3 pct with no data available from NBS on the value of σ. However, a comparison of the measured value of tanδ of quartz was found (*4*), which gave a comparative error of 2.5 pct. With the small loss approximation (tanδ << 1) and calculating σ by an iterative process involving ϵ_r, the error should be within the same ±3 pct of ϵ_r.

MINERAL PROPERTIES

The minerals in this report have been selected to give a broad coverage of those that are encountered in natural ores. They represent both the valuable and nonvaluable mineral constituent of ores.

Measurements have been taken on several classes of minerals which are grouped according to their chemical composition and consist of six groups: (1) oxides, (2) carbonates, (3) silicates, (4) phosphates and sulfates, (5) haloids, and (6) tungstates. (tables 3-8). These minerals represent the dielectric property trends that could be encountered with an expanded sample list, and are some of the more frequently encountered minerals that are of interest in extractive metallurgy. These are relatively low-conductive minerals to which the theory of measurement only applies. High-loss minerals are therefore omitted from this tabulation.

Because the composition of each mineral can vary and the minerals may have some impurities, appendix B is added to show the chemical composition of each mineral, its purity analysis, and the location of the source of the mineral sample.

The measured values of the dielectric properties of the mineral samples were made at room temperature. The conductivity is highly temperature dependent and can change while a mineral is being heated. The dielectric property measurements were taken at 100 MHz intervals, beginning at 300 MHz and ending at 1 GHz.

TABLE 2. - Comparison of measured dielectric properties with published data

Mineral	Dielectric constant, (ϵ_r)			Loss tangent (tanδ)		
	Measured value	Reference value[1]	Difference, pct	Measured value	Reference value[1]	Difference, pct
Quartz	3.90	3.85	1.3	1.56×10^{-4}	1.6×10^{-4}	2.5
Corundum	9.0	9.34	2.57	1.30×10^{-4}	NA	NA
Calcite	8.87	8.60	3.14	5.56×10^{-5}	NA	NA
Periclase	9.41	9.65	2.49	4.52×10^{-5}	NA	NA

NA Not Available

[1]All from Young (*4*).

TABLE 3. - Measured dielectric properties for mineral group oxides

(All values of the loss tangent (tanδ) are multiplied by 10^{-4})

Frequency, MHz	*300*	*400*	*500*	*600*	*700*	*800*	*900*	*1,000*
Bauxite:								
ϵ_r	6.75	6.39	6.01	5.92	5.93	6.36	6.40	6.46
tanδ	1.98	2.13	2.11	2.25	6.04	2.61	2.53	1.87
Chromite:								
ϵ_r	11.35	11.26	11.69	11.36	10.78	10.98	11.22	10.96
tanδ	2.36	ND	1.69	1.34	1.69	2.08	1.63	1.45
Columbite:								
ϵ_r	25.03	26.97	26.19	25.89	26.47	24.82	26.21	25.24
tanδ	11.80	5.43	11.40	5.86	ND	5.68	ND	6.18
Corundum:								
ϵ_r	10.25	10.21	10.20	10.19	10.26	10.03	9.95	9.81
tanδ	ND	3.23	1.11	.66	.57	1.36	1.28	1.86
Goethite:								
ϵ_r	10.44	9.40	9.52	10.44	10.08	9.58	9.60	8.94
tanδ	2.60	2.67	2.97	2.96	2.11	2.59	4.82	3.98
Periclase:								
ϵ_r	9.80	9.54	9.61	9.70	9.36	9.24	9.45	9.58
tanδ	.56	.69	.68	.57	.41	ND	ND	3.35

ND Not determined.

TABLE 4. - Measured dielectric properties for mineral group carbonates

(All values of the loss tangent (tanδ) are multiplied by 10^{-4})

Frequency, MHz	*300*	*400*	*500*	*600*	*700*	*800*	*900*	*1,000*
Aragonite:								
ϵ_r	8.31	8.16	8.11	8.38	8.30	8.16	8.18	8.25
tanδ	1.29	1.50	1.37	1.06	1.00	1.47	1.20	0.98
Calcite:								
ϵ_r	9.16	8.89	9.10	8.86	9.02	8.66	8.84	8.91
tanδ	.77	.87	.67	.62	.33	.84	ND	.47
Cerussite:								
ϵ_r	22.24	23.61	21.96	23.62	21.89	22.98	22.66	22.98
tanδ	2.00	.93	1.45	ND	ND	6.54	ND	15.80
Dolomite:								
ϵ_r	7.62	7.38	7.32	7.37	7.34	7.22	7.26	7.41
tanδ	2.60	2.98	2.51	3.39	4.34	2.63	3.11	2.42
Magnesite:								
ϵ_r	6.85	6.71	6.59	6.63	6.74	6.64	6.61	6.61
tanδ	2.59	1.81	1.51	1.58	1.47	1.89	1.57	1.21
Malachite:								
ϵ_r	6.97	6.87	6.76	6.81	6.69	6.63	6.65	6.81
tanδ	2.13	2.40	1.87	1.92	1.90	2.27	2.17	2.06
Rhodochrosite:								
ϵ_r	8.69	8.59	8.56	8.83	8.44	8.26	8.26	8.32
tanδ	3.62	3.09	3.71	3.90	4.79	7.18	7.01	5.28
Siderite:								
ϵ_r	7.50	7.16	7.20	7.64	7.41	7.04	7.10	7.41
tanδ	1.92	2.69	2.76	1.79	1.20	2.35	2.67	1.69
Smithsonite:								
ϵ_r	9.99	9.65	9.86	9.91	9.47	9.35	9.58	9.61
tanδ	1.19	1.37	1.34	1.20	1.03	1.23	2.15	1.06
Witherite:								
ϵ_r	7.55	7.30	7.23	7.43	7.30	7.02	7.01	7.32
tanδ	1.14	1.27	1.44	.91	.69	1.63	4.32	.78

ND Not determined.

TABLE 5. - Measured dielectric properties of silicates

(All values of the loss tangent (tanδ) are multiplied by 10^{-4})

Frequency, MHz	*300*	*400*	*500*	*600*	*700*	*800*	*900*	*1,000*
Beryl:								
ϵ_r	6.74	6.47	6.46	6.83	6.76	6.43	6.38	6.59
tanδ	0.33	0.27	2.58	1.01	0.71	ND	1.89	8.39
Biotite:								
ϵ_r	6.83	6.25	5.94	5.84	5.39	5.91	5.61	5.90
tanδ	4.46	4.19	4.62	4.70	6.05	4.56	1.05	3.46
Kyanite:								
ϵ_r	9.01	8.85	8.68	8.90	8.59	8.47	8.67	8.74
tanδ	.90	.98	ND	ND	.29	.96	.87	.35
Lepidolite:								
ϵ_r	5.28	5.00	4.84	4.93	4.96	4.91	4.95	5.15
tanδ	1.43	1.45	2.72	1.62	1.30	1.89	2.36	.88
Muscovite:								
ϵ_r	4.08	4.01	3.97	4.10	4.40	4.36	4.23	4.46
tanδ	5.33	3.37	4.44	4.42	1.93	2.26	1.79	7.54
Nephelene:								
ϵ_r	7.03	6.99	6.74	6.66	6.68	6.80	6.71	6.57
tanδ	1.27	1.45	1.44	1.42	1.94	2.01	.80	.89
Orthoclase:								
ϵ_r	4.56	4.54	4.43	4.37	4.40	4.41	4.37	4.34
tanδ	.64	.47	ND	.64	.63	ND	ND	.43
Pollucite:								
ϵ_r	5.88	5.99	6.02	6.09	6.14	6.02	5.95	6.08
tanδ	2.83	2.08	1.36	1.10	1.41	1.70	1.47	.92
Quartz:								
ϵ_r	4.00	3.96	3.89	3.85	3.90	3.97	3.94	3.89
tanδ	1.88	1.50	2.20	1.82	1.54	ND	1.60	1.37
Sericite:								
ϵ_r	6.73	6.46	6.24	6.30	6.10	5.99	6.08	6.20
tanδ	1.09	.78	.62	.77	.74	1.37	1.64	.68
Spodumene:								
ϵ_r	7.25	7.11	6.98	7.04	7.07	7.03	6.95	6.98
tanδ	1.76	1.74	1.54	1.16	.99	1.49	1.32	1.04
Tourmaline:								
ϵ_r	5.40	5.44	4.23	4.96	5.00	5.19	5.29	5.21
tanδ	.79	2.09	2.41	2.16	2.38	2.08	1.02	2.55

ND Not determined.

TABLE 6. - Measured dielectric properties of phosphates and sulfates

(All of the loss tangents (tanδ) are multiplied by 10^{-4})

Frequency, MHz	*300*	*400*	*500*	*600*	*700*	*800*	*900*	*1,000*
Anhydrite:								
ϵ_r	6.46	6.20	6.14	6.34	6.40	6.22	6.09	6.27
tanδ	1.18	1.54	1.71	1.14	0.84	ND	ND	0.97
Apatite:								
ϵ_r	9.65	8.97	9.21	9.64	9.14	8.85	9.39	9.43
tanδ	.37	.51	.68	.58	.58	ND	.70	.81
Barite:								
ϵ_r	9.62	9.35	9.54	9.69	9.41	9.14	9.48	9.52
tanδ	.63	1.14	1.02	.60	ND	3.31	1.07	.61
Celestite:								
ϵ_r	11.52	11.29	11.58	11.45	11.03	11.15	11.36	11.23
tanδ	.37	.27	ND	.39	.39	ND	ND	.49
Monazite:								
ϵ_r	12.44	12.28	12.39	12.42	12.42	12.53	12.34	12.13
tanδ	1.51	1.47	1.07	.85	1.75	1.39	1.19	.93

ND Not determined.

TABLE 7. - The measured dielectric properties of haloids

(All values of the loss tangent (tanδ) are multiplied by 10^{-4})

Frequency, MHz	300	400	500	600	700	800	900	1,000
Cryolite:								
ϵ_r	6.78	6.62	6.56	6.61	6.67	6.45	6.33	6.45
tanδ	4.36	ND	4.15	5.07	2.57	3.92	4.11	4.02
Flourithe:								
ϵ_r	6.55	6.46	6.41	6.59	6.59	6.52	6.44	6.58
tanδ	.59	.64	1.22	.85	.57	ND	ND	.73
Halite:								
ϵ_r	4.96	5.05	5.06	4.95	4.81	4.87	4.89	4.83
tanδ	1.07	1.23	1.45	1.01	.79	ND	ND	.92

ND Not determined.

TABLE 8. - Measured dielectric properties of tungstates

(All values of the loss tangent (tanδ) are multiplied by 10^{-4})

Frequency, MHz	300	400	500	600	700	800	900	1,000
Scheelite:								
ϵ_r	10.50	10.01	10.75	10.76	10.12	10.27	10.69	10.50
tanδ	0.94	0.65	0.70	0.91	0.55	1.01	1.32	1.08
Wolframite:								
ϵ_r	15.90	16.08	15.86	15.33	15.50	15.68	15.53	15.93
tanδ	ND	ND	ND	2.45	ND	2.57	2.50	.94

ND Not determined.

MICROWAVE HEATING STUDIES

After the dielectric properties of each mineral were measured, microwave heating studies were conducted. From these studies it could be determined if the amount of microwave energy absorbed by a mineral could be predicted by knowing its dielectric properties and the amount of microwave energy available.

First, a theoretical heating model was developed through electromagnetic theory that would predict the amount of microwave energy that could be absorbed by a mineral. This heating model could be expressed in terms of known quantities (available power, frequency, microwave waveguide dimensions, etc.) and the measured dielectric properties for each mineral.

Second, the minerals were actually irradiated with microwave energy and actual heating studies were conducted, thus the absorbed power could be calculated from measured heating and cooling rates, and temperature changes in the mineral using a heating model developed from classical thermodynamics. Finally, the results of these two models were compared for each mineral.

The following sections will further explain each of the preceding models and present a summary of results.

DIELECTRIC HEATING MECHANISMS

In order to understand the behavioral characteristics of a mineral placed in an electromagnetic field (microwave), it is necessary to understand the concepts involved in dielectric heating. Minerals can be classified as conductors, insulators, and absorbers. Figure 6 illustrates the effects of microwave radiation on each classification.

Microwaves behave with the same characteristics as light waves. Both are electromagnetic energy traveling at the speed of light, but at different frequencies. Both waves can be reflected off materials, transmitted through materials, or absorbed by materials. However, no material is a perfect conductor or insulator and therefore absorbs electromagnetic energy to some degree. This degree is based upon the dielectric properties of each material.

When a mineral is placed in an electric field, the polarizability of the mineral is affected. The total polarization can be expressed as the sum of the four dominant mechanisms (*19*),

$$\alpha_p = \alpha_{e\ell} + \alpha_{ion} + \alpha_{dip} + \alpha_{int}, \qquad (12)$$

where α_{el} is the electronic contribution and results from the displacement of the electron cloud relative to the nucleus, α_{ion} is the ionic effect component and results from the movement of one ion with respect to other ions in the presence of an electric field, α_{dip} originates from the presence of permanent dipoles in the host lattice commonly referred to as orientational polarization, and α_{int} originates from random or layered inhomogeneities and is commonly referred to as interfacial polarization.

Figure 7 depicts these mechanisms that are usually pronounced at certain frequency realms (*20*).

In the microwave spectrum, the primary heating mechanism is the orientational mode of the molecule

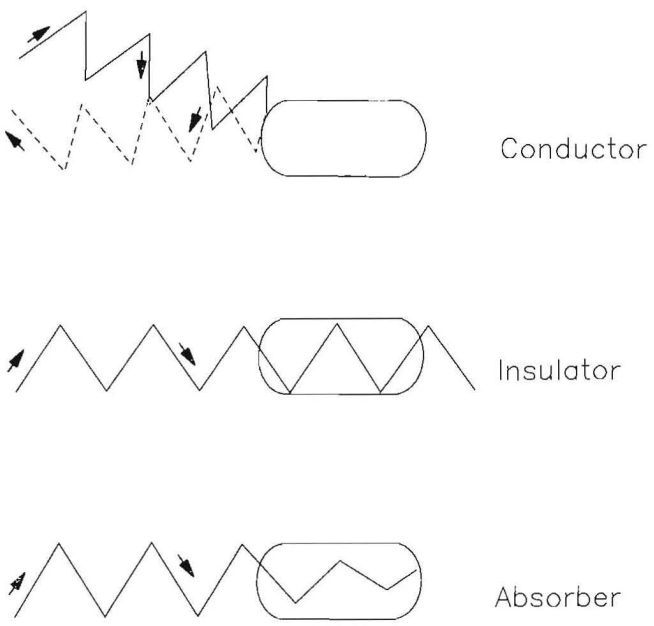

Figure 6. - Microwave absorption characteristics for conductor, insulator, and absorber.

(dipole orientation of the Debye type, i.e. relaxational). Highly polar molecules, such as the water molecules shown in figure 8, will tend to align themselves with the electric field. This process is quite rapid and occurs 1.8 x 10^9 times a second at the frequency of 915 MHz. The rapid movement of the molecules results in kinetic energy, which can be measured as heat and is proportional to the dielectric loss factor, ϵ'' (the product of ϵ_r and $\tan\delta$).

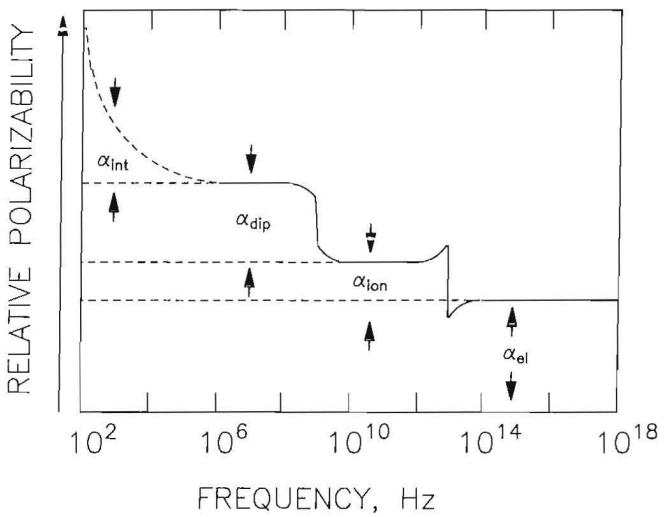

Figure 7. - Effects of frequency on mechanisms that affect polarizability.

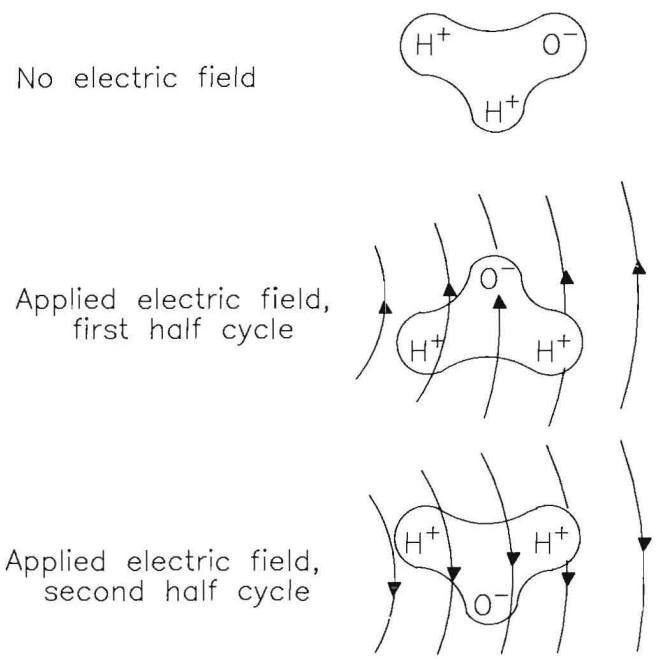

Figure 8. - Dipole polarization example of water molecule.

THEORETICAL HEATING MODEL BASED UPON MICROWAVE THEORY

The dynamics of incident electromagnetic waves have been derived from Maxwell's equations, which predict the dielectric response of a material exposed to an electric field. As previously mentioned, the presence of an electric field on a dielectric polarizes the material resulting in kinetic energy measured as heat. This heat can be expressed in terms of the absorbed power density, P_d, by the relation

$$P_d = \omega E_0^2 \epsilon \tan\delta \qquad (13)$$

where ω = $2\pi f$, rad/s,

f = frequency, Hz,

E_o = magnitude of electric field, V/cm,

ϵ = $\epsilon_r \cdot \epsilon_o$, F/cm,

ϵ_o = permittivity of free space
= 8.854×10^{-14}, F/cm,

ϵ_r = dielectric constant,

and $\tan\delta$ = loss tangent of material.

Rearranging equation (13) yields

$$P_d = kfE_o^2 \epsilon_r \tan\delta, \qquad (14)$$

where k = $2\pi\epsilon_o$ = 55.63×10^{-14}, F/cm.

From equation 14, the amount of power absorbed by a material in an electric field is proportional to the dielectric properties of the material; namely ϵ_r and $\tan\delta$.

In each heating experiment, the mineral samples were placed inside a WR 975 waveguide that was shorted at the end. To determine a value for E_o in equation 14 for these purposes, the electric field wave propagation in a rectangular waveguide must be examined.

The electric field strength, E_t, for a union traveling wave is given by

$$E_t^2 = 2\eta_g P_d \qquad (15)$$

where η_g is the intrinsic impedance in the waveguide and P_d is the power density at the sample in watt per square centimeter (*21*, p. 397).

But in a WR 975 rectangular waveguide and at the frequency of 915 MHz, the only mode of excitation is the TE_{10} (transverse electric) mode, thus the traveling electric field, E_t, can be written as,

$$E_t = E_p \cos \frac{\pi x}{a}$$

for $$-\frac{a}{2} < x < \frac{a}{2} \quad (16)$$

where a = width of waveguide,
x = any distance along 'a' measured from center of guide,

and E_p = peak electric field intensity.

By averaging the electric field across the waveguide,

$$|E_p|^2 = 2\,|E_t|^2. \quad (17)$$

The relationship between the traveling electric field and the standing wave of the electric field with the waveguide shorted at the end is,

$$|E_s| = 2\,|E_t|. \quad (18)$$

where E_s is the standing wave of the electric field (*21*, p. 409).

Also, at a peak of the traveling wave

$$|E_{ps}| = 2\,|E_{pt}| \quad (19)$$

where E_{ps} is the peak electric field of the standing wave and E_{pt} is the peak traveling wave.

From equations 17 through 19,

$$|E_{ps}|^2 = 4\,|E_{pt}|^2 = 8\,|E_t|^2. \quad (20)$$

Substituting equation (20) into equation (15) gives the relation,

$$|E_{ps}|^2 = 16\,\eta_g\,P_d. \quad (21)$$

In the experimental procedures of heating the mineral samples, a WR 975 rectangular waveguide was short circuited to ensure a null of the electric field at the end of the guide. The mineral sample was placed three fourths of a guide wavelength from the short circuit at the position of a peak of the standing wave of the electric field. Figure 9 depicts the location of the sample in the waveguide. Because the guide was short circuited, a standing wave, two times greater than the traveling wave, is obtained at the location where the mineral sample will be placed in the waveguide, thus equation 21 is used to calculate the electric field strength at the mineral sample.

since $$\eta_g = \frac{\lambda_g}{\lambda_o}\,\eta_o \quad (22)$$

and $$\lambda_g = \frac{\lambda_o}{\sqrt{1 - (f_c/f)^2}} \quad (23),$$

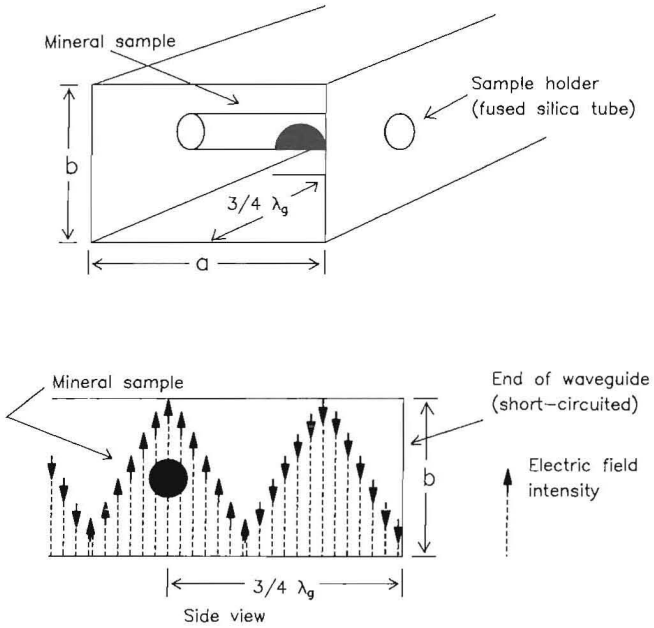

Figure 9. - Orientation of mineral sample in microwave waveguide during irradiation studies.

where η_o = intrinsic impedance of free space = 377 Ω,

λ_o = free space wavelength = c/f, cm,

c = speed of light = 3.00×10^{10} cm/s,

f = frequency = 915 MHz,

λ_g = wavelength in guide, cm,

and f_c = cutoff frequency for waveguide = c/2a = 605.8 MHz,

and making the proper substitutions into equations 21, 22, and 23, the relationship between the electric field strength and the applied power, P_a, in watts becomes

$$|E|^2 = 26.2\,P_a, \quad (24)$$

where P_a is equal to P_d times the width and height of the waveguide. Substituting this value of E into equation 14 allows the theoretical power absorbed by the mineral to be computed.

ACTUAL HEATING MODEL BASED UPON THERMODYNAMICS

In order to compare the microwave power actually absorbed by the sample with the power absorption predicted by the theoretical model, a mathematical model for the heating of a low-loss material was developed. This model assumes that, for small rises in temperature, the

sample loses heat primarily by convection and conduction, therefore, its radiant heat loss may be neglected. It is also assumed that the thermal and electrical properties of the material are constant over the range of temperatures of interest and that the ambient temperature, according to the first law of thermodynamics, is given by

$$dT/dt = (P/C_p\rho) - C_o (T-T_o), \quad (25)$$

where P = absorbed power, cal • s^{-1} • cm^{-3},

C_p = specific heat, cal • g^{-1} • $°C^{-1}$,

ρ = density, g • cm^{-3},

T = sample temperature, °C,

T_o = ambient temperature, °C,

and C_o = constant that depends on the thermal conductivity and geometry of the sample.

Equation 25 can also be written as

$$\left(\frac{dT}{dt}\right)_{heating} = -C_oT + R_c \quad (26)$$

where $$R_c = \frac{P}{C_p\rho} + C_oT_o \quad (27)$$

is a constant.

When the microwave power is turned off; P=O, the sample cools according to the relation

$$\left(\frac{dT}{dt}\right)_{cooling} = -C_o(T - T_o). \quad (28)$$

Equations 26 and 28 predict that both the heating and cooling curves should be exponential and that on heating the sample, the temperature should asymptotically approach a limiting temperature, T_f,

where $$T_f = \frac{P}{C_oC_p\rho} + T_o. \quad (29)$$

Unfortunately P can not be determined directly from equation 29 by measuring T_f since for long-term heating, T_o slowly increases because of transfer of heat from the sample to the gas filling the waveguide and to the walls of the guide itself. It was therefore necessary to determine P from the simultaneous solution of equations 26 and 28. T was measured as a function of time for both the heating and the cooling. A computer program was written that determined the slope of these curves as a function of T. A linear regression of $(dT/dt)_{cooling}$ versus T allowed the value of the constants C_o and T_o to be determined, and a regression of $(dT/dt)_{heating}$ versus T allowed the value of R to be determined. These values were then substituted into equation 27 to find P.

The heating model can be expected to give meaningful results only under conditions where the assumption under which it was derived are valid. To insure this, the total temperature rise must be kept small, probably well under 100°C. For larger changes in temperature the ϵ_r, $\tan\delta$, and thermal conductivity can not be considered constants. Also at high temperatures, radiation loss, which varies as the fourth power of temperature, becomes the dominant thermal loss mechanism. These factors all cause departures from the idealized exponential heating curves. This implies that the model is applicable only to relatively low-loss materials and that heating times must be kept short so that changes in ambient temperature within the guide will not effect the results.

As discussed below, the exponential heating and cooling approximation proved to be reasonably good for low-loss materials and short heating times. As expected, however, highly absorbing materials displayed marked deviations from this exponential curve and frequently exhibited sudden changes in the heating rate that were attributed to phase changes and/or the onset of chemical reactions in the sample.

THERMAL RESPONSE

Studies of the actual power absorbed by each mineral were conducted utilizing a 915 MHz microwave generator. The mineral sample was placed in the center of a WR 975 waveguide, which was short circuited at one end, which in turn produced a null of the electric field at the end of the waveguide. Figure 10 shows the end of the waveguide where the mineral samples were heated and tested. The sample was placed three-fourths of a wavelength from the short (at a maximum of the standing wave). Figure 11 shows the microwave generator, controls, and associated waveguide and heating chamber.

These tests were conducted in an inert atmosphere where the applied power from the microwave generator was 15 kW. A thermocouple was placed inside the waveguide on the mineral sample to measure its temperature during the heating and cooling process. The thermocouple was silver-plated to limit absorption and was placed perpendicular to the electric field to further minimize heating errors.

The temperature was recorded by a computer at 2-s intervals for a total heating cycle of slightly less than 2 min. This allowed the sample to reach a steady state temperature at which time the power was terminated and the sample allowed to cool. Figure 12 shows a typical heating curve for a mineral sample.

Each mineral, whose dielectric properties were measured earlier, was heated in the microwave generator as described above. Heating and cooling rates of each mineral were measured and the absorbed power was calculated by the equations presented in the actual heating model.

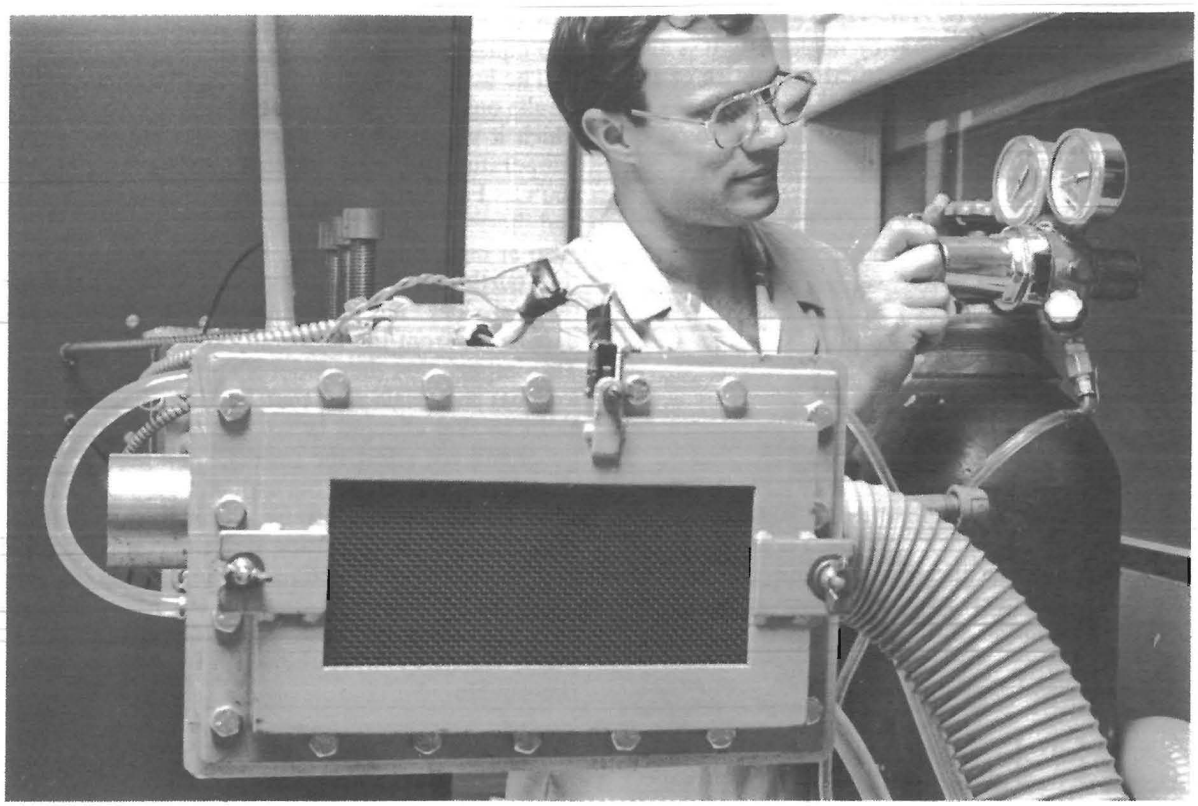

Figure 10. - Microwave waveguide being readied for dielectric heating test.

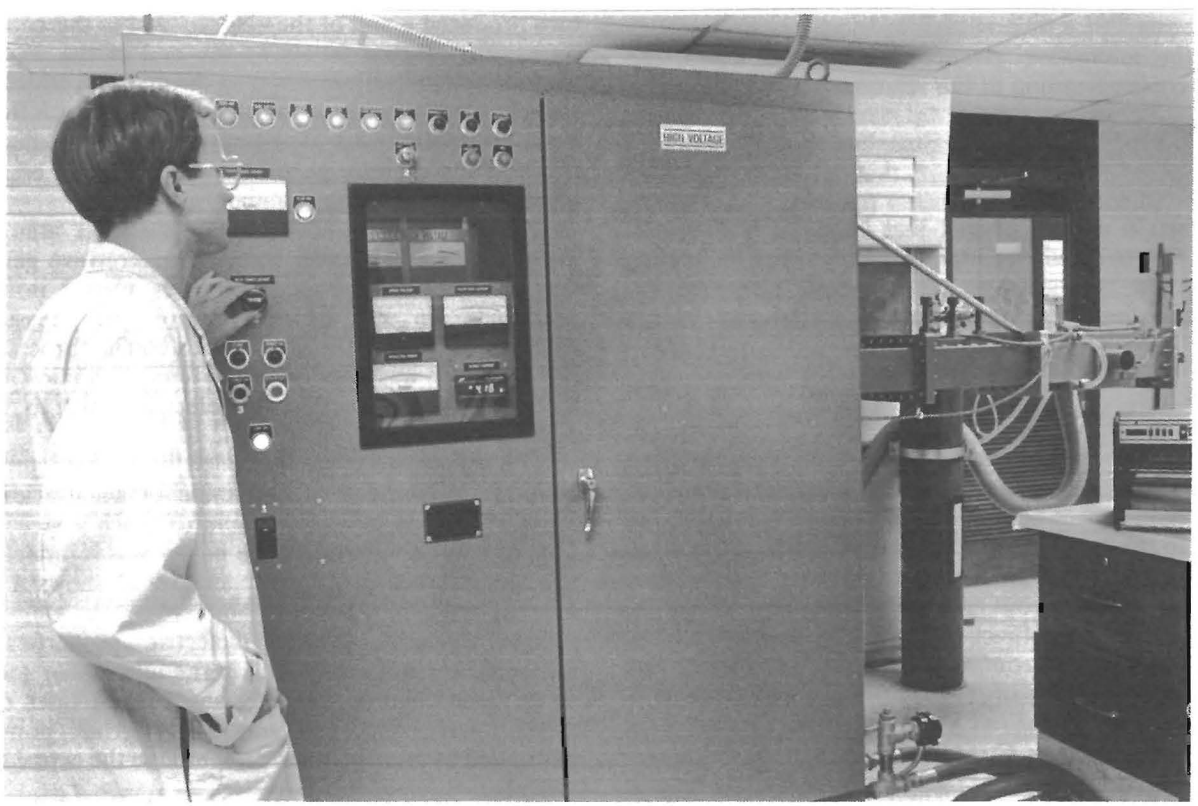

Figure 11. - Microwave generator apparatus.

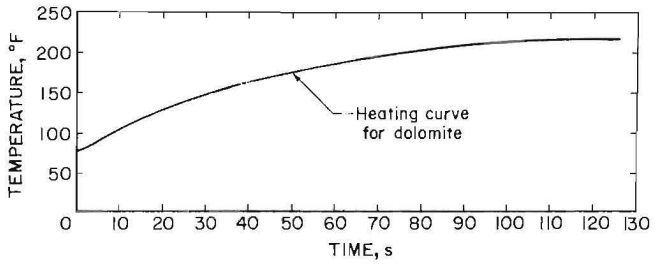

Figure 12. - Typical dielectric heating curve for mineral dolomite.

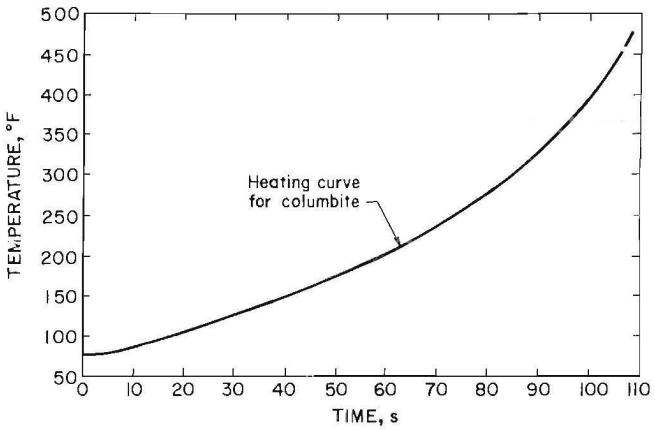

Figure 13. - Thermal runaway curve of columbite.

PERFORMANCE

Comparison studies of actual power absorption versus theoretical power absorption were conducted for each mineral and the results are presented in table 9. Columns 2 and 3 in table 9 represents the dielectric properties of each mineral measured at 915 MHz by the technique described earlier. Column 4 of table 9 represents the theoretical power absorbed by each mineral, which was determined by the method discussed in the section "Theoretical Heating Model Based Upon Microwave Theory". The computed value of the theoretical electric field strength at the location of the mineral sample inside the waveguide given in equation 24 resulted in 600 V/cm for an applied power of 15 kW. This value of the electric field strength along with the dielectric properties of each mineral were used in equation (13) to calculate the theoretical absorbed power. The actual absorbed power was then computed through equations 26 through 29 and the results are tabulated in column 3.

As previously mentioned, dielectric properties are temperature dependent and usually increase with temperature. A problem of thermal runaway can be encountered whenever a material absorbs microwave energy in excess of its critical temperature. Critical temperature can be defined as that temperature which

TABLE 9. - Electrical property measurements of minerals at the conventional microwave frequency (915 MHz) with power absorption calculations

	Dielectric property measurements		*Power absorption, W/cm²*	
Minerals	*Dielectric constant* ϵ_r	*Loss tangent,* $\tan\delta \times 10^{-4}$	*Actual*	*Theoretical*
Anhydrite	6.27	0.972	0.1416	0.120
Apatite	9.39	.697	.279	.129
Aragonite	8.18	1.20	.506	.193
Barite	9.48	1.07	.108	.199
Bauxite	6.40	2.53	.691	.318
Beryl	6.38	1.89	.129	.237
Biotite	5.61	1.05	.006	.116
Calcite	8.91	.466	.078	.082
Celestite	11.23	.486	.013	.107
Cerussite	22.98	4.570	.295	2.052
Chromite	11.22	1.63	.563	.359
Columbite	25.24	6.18	.887	3.07
Corundum	9.81	.734	.192	.141
Cryolite	6.33	4.11	.34	.511
Dolomite	7.26	4.32	.639	.616
Fluorite	6.58	.734	.083	.094
Goethite	9.60	4.82	1.69	.909
Halite	4.83	.920	.18	.087
Kyanite	8.65	.386	.064	.066
Lepidolite	4.95	2.36	.198	.230
Magnesite	6.61	1.57	.611	.204
Malachite	6.65	2.17	.550	.284
Monazite	12.34	1.19	.271	.289
Muscovite	4.23	1.79	.128	.149
Nephelene	6.71	.800	.438	.105
Orthoclase	4.34	.429	.076	.037
Periclase	9.45	.452	.043	.084
Pollucite	5.95	1.47	.333	.172
Quartz	3.94	1.60	.120	.124
Rhodochrosite	8.26	7.01	.234	1.14
Scheelite	10.69	1.32	.209	.277
Sericite	6.08	1.64	.17	.196
Siderite	7.10	2.67	.414	.373
Smithsonite	9.58	2.15	.55	.405
Sphalerite	9.66	7.36	.113	1.40
Spodumene	6.95	1.32	.204	.180
Tourmaline	5.29	1.02	.314	.106
Witherite	7.01	4.32	.295	.595
Wolframite	15.53	2.50	1.17	.762

represents an upper limit beyond which heating can become unstable, whatever the heat transfer mechanism (*20*). Figure 13 is an example of the thermal runaway condition encountered while testing columbite in the microwave waveguide. This condition can be prevented by controlling either the power intensity or the heat transfer mechanism. In either case, a heat evacuation technique with respect to time is the end result. Columbite was the only mineral encountered that exhibited this exponential heating during the test sequence. It is anticipated that this phenomenon will be encountered more frequently with the higher loss materials.

CONCLUSIONS

Basic dielectric property data have been collected on some of the more common low-loss minerals. Though far from complete, these data can give a relative prediction of how a material will be affected by microwave radiation, even if, the loss tangent is highly temperature dependent, which results in a change of the dielectric loss factor as the temperature of the mineral increases. A knowledge of the temperature relationships to the dielectric properties and an improved heating model incorporating these relationships should give closer agreement between the theoretical heating model data and the actual heating data. For low-loss minerals the theoretical heating model can be used to predict the amount of microwave absorption.

A general indication could be assumed from the mineral classification system that most nonmetallic oxides, carbonates, and silicates are relatively low-loss minerals, therefore, microwave absorption is low.

The dielectric property data are presented in appendix A, which depicts the relationship among the dielectric constant, conductivity, and the loss tangent values as measured through the frequency range of 300 MHz to 1 GHz. These data cover the frequency range for the 915-MHz generator, but represents a small fraction of the microwave spectrum.

The general trend of the conductivity of the mineral is increasing with higher frequency as can be seen from the plotted data in appendix A. This being the case, improved absorption frequency bonds probably exist for some minerals in the higher frequency realms prior to the ionizing radiation regions in the infrared spectrum. Additional research is required in this area to determine the maximum absorption band in the microwave spectrum as this research was limited to the lower regions of the spectrum.

The utilization of microwave heating methods combined with pyrometallurgical processing may provide for fast, efficient heating where required for mineral beneficiation. As can be seen from tables 3 through 8, some minerals are the primary gangue constituent. Where it is desirable to heat a mixture of two or more materials, the rate of heating will depend upon the dielectric properties of each.

Different heating rates will then occur and in many cases this effect can be used to selectively modify the chemical or physical properties of one of the constituents, thereby enhancing the potential for mineral separation.

REFERENCES

1. Wagman, D. D., W. H. Evans, V. B. Parker, R. H. Schumm, I. Halow, S. M. Bailey, K. L. Churney, and R. L. NuHall. The NBS Tables of Chemical Thermodynamic Properties. J. Phys. Chem. Ref. Data., v. 2, No. 2, 1982, 391 pp.

2. Pankratz, L. B., J. M. Stuve, and N. A. Gokcen. Thermodynamic Data for Mineral Technology. BuMines B 677, 1985, 355 pp.

3. Parkhomenko, E. I. Electrical Properties of Rocks. Plenum, 1967, 314 pp.

4. Young, K. F., and H. P. R. Frederikse. Compilation of the Static Dielectric Constant of Inorganic Solids. J. Phys. Chem. Ref. Data., v. 2, No. 2, 1973, pp. 313-410.

5. Von Hippel, A. R. (ed.). Dielectric Materials and Applications. Papers by Twenty-Two Contributors. MIT Press, 1966, 425 pp.

6. Morgan, S. O., D. Edelson, W. McMahan, and W. J. Merz. Properties of Dielectrics. Ch. in American Institute of Physics Handbook, ed. by D. E. Gray. McGraw-Hill, 5th ed., 1957, pp. 5-114–5-117.

7. Dana, E. S., and W. E. Ford. Dana's Manual of Mineralogy. Wiley, 16th ed., 1952, 530 pp.

8. Cook, J. C. RF Electrical Properties of Bituminous Coal Samples. Geophys. v. 35, No. 6, Dec. 1970, pp. 1079-1085.

9. Geyer, R. G., G. V. Keller, and T. Ohya. Research on the Transmission of Electromagnetic Signals Between Mine Workings and the Surface (contract No. H0101691), BuMines OFR 61-74, Jan. 10, 1974, 124 pp., NTIS PB 237852.

10. LaGace, R. L., J. M. Dobbie, T. E. Deerfler, W. S. Hawes, and R. H. Spencer. Antenna Technology for Medium Frequency Portable Radio Communication in Coal Mines. Paper in Electromagnetic Guided Waves in Mine Environments. Proceeding of a workshop (contract H0155008, U.S. Dep. Commerce. BuMines OFR 134-78, 1978, pp. 153-169.

11. Rubin, L. A., and J. C. Fowler. Ground Probing Radar for Delineation of Rock Features. Eng. Geol. (Amsterdam), v. 12, No. 2, July 1978, pp. 163-170.

12. Balancis, C. A., W. S. Rice, and N. S. Smith. Microwave Measurements of Coal. Radio Sci., v. 11, No. 4, Apr. 1976, pp. 413-418.

13. Cook, J. C. An Electrical Crevasse Detector. Geophysics, v. 21, No. 4, 1956, pp. 1055-1070.

14. ____. Seeing Through Rock With Radar. Paper in Proc. of the 1st North American Rapid Excavation and Tunneling Conf. AIME, v. 1, ch. 9, 1972, pp. 89-101.

15. Church, R. H., W. E. Webb, and J. R. Boyle, Jr. Ground-Penetrating Radar for Strata Control. BuMines RI 8954, 1985, p. 16.

16. Jordan, C. E., and G. V. Sullivan. Dielectric Separation of Minerals. BuMines B 685, 1986, p. 17.

17. Hayt, W. H., Jr. Engineering Electromagnetics. McGraw-Hill, 1981, pp. 433-439.

18. Webb, W. E., and R. H. Church. Measurement of Dielectric Properties of Minerals at Microwave Frequencies. BuMines RI 9035, 1986, 8 pp.

19. Taggart, G. B. Electromagnetic Processing of Materials. Contract Rep. MPA 903-84-C-0039, Def. Adv. Res. Projects Agency, Dep. Def., Feb. 6 - Aug. 17, 1984, by BDM Corp., McLean, VA, p. III-1–III-14.

20. Roussy, G., A. Mercier, J. M. Thiebaut, and J. P. Vanbourg. Temperature Runaway of Microwave Heated Materials: Study on Control. J. Microwave Power, v. 20, No. 1, 1985, pp. 47-51.

21. Hayt, W. H., Jr. Engineering Electromagnetics. McGraw-Hill, 1981, 512 pp.

22. Brown, R. G., R. A. Sharpe, W. L. Hughes, and R. E. Post. Lines, Waves and Antennas. The Transmission of Electric Energy. John Wiley and Sons, New York, 1973, 2nd ed., p. 239.

APPENDIX A.–MEASURED DIELECTRIC PROPERTIES OF LOW-LOSS MINERALS

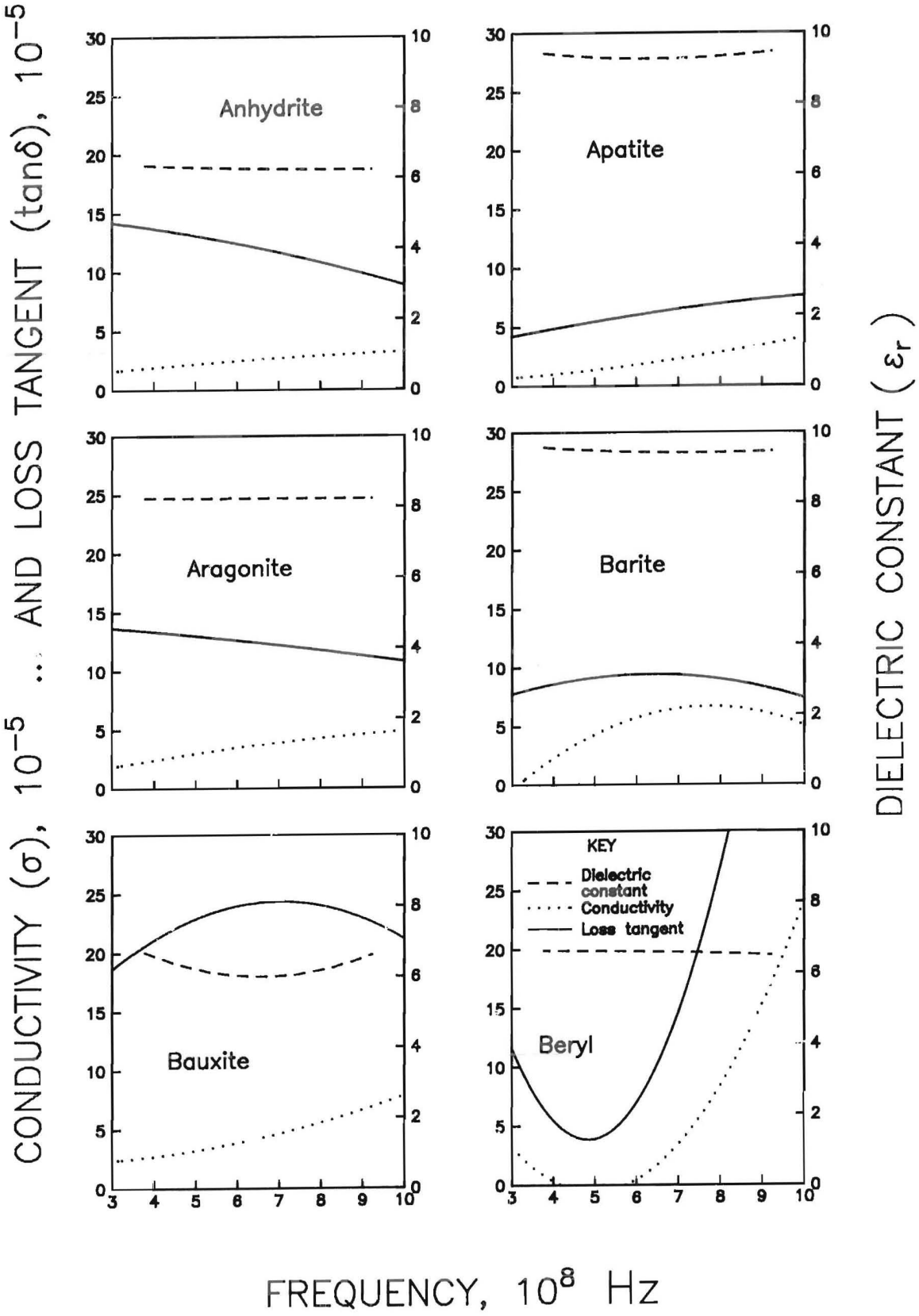

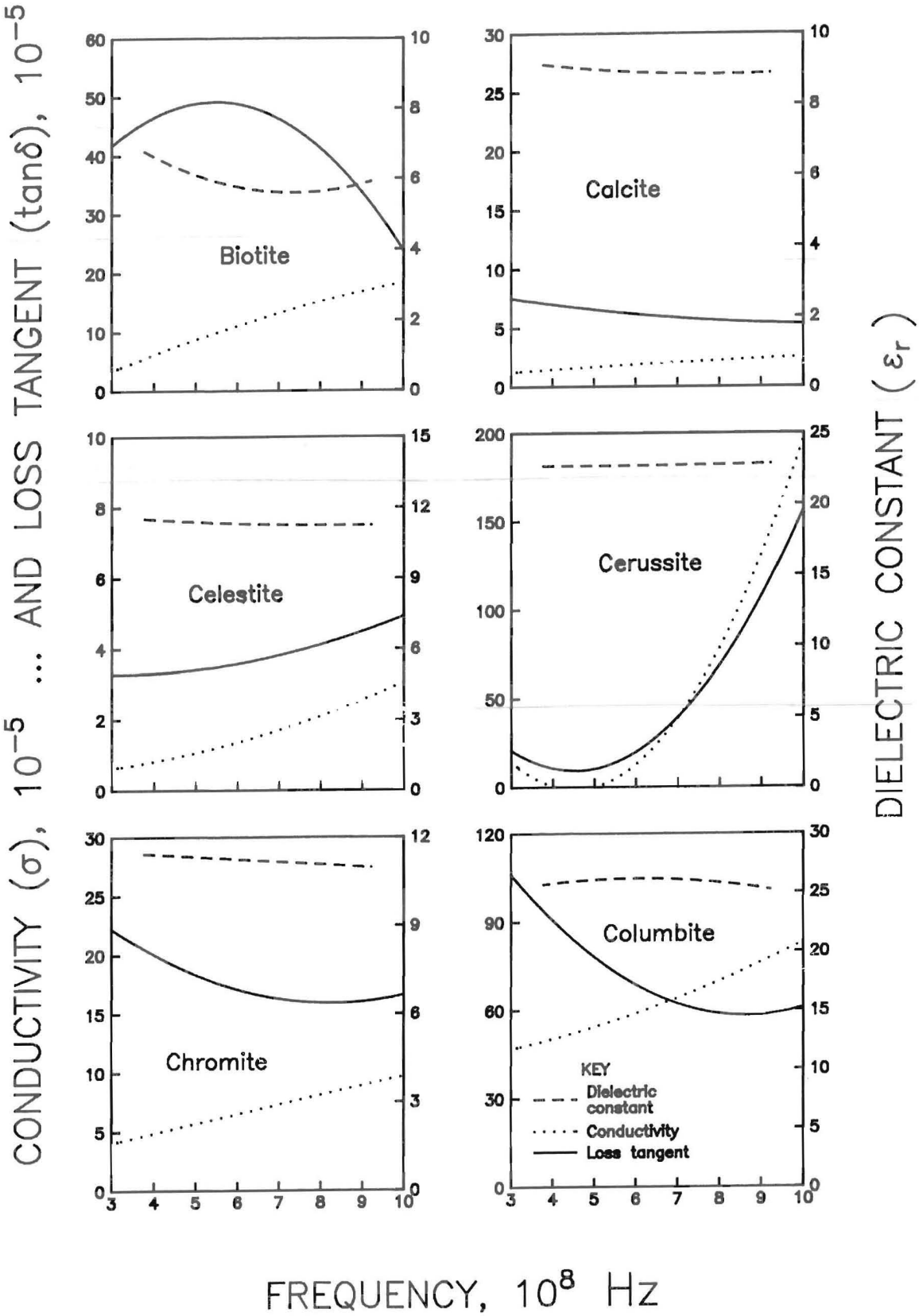
CONDUCTIVITY (σ), 10⁻⁵ ... AND LOSS TANGENT (tanδ), 10⁻⁵
DIELECTRIC CONSTANT (εr)
Biotite
Calcite
Celestite
Cerussite
Chromite
Columbite
KEY
Dielectric constant
Conductivity
Loss tangent
FREQUENCY, 10⁸ Hz

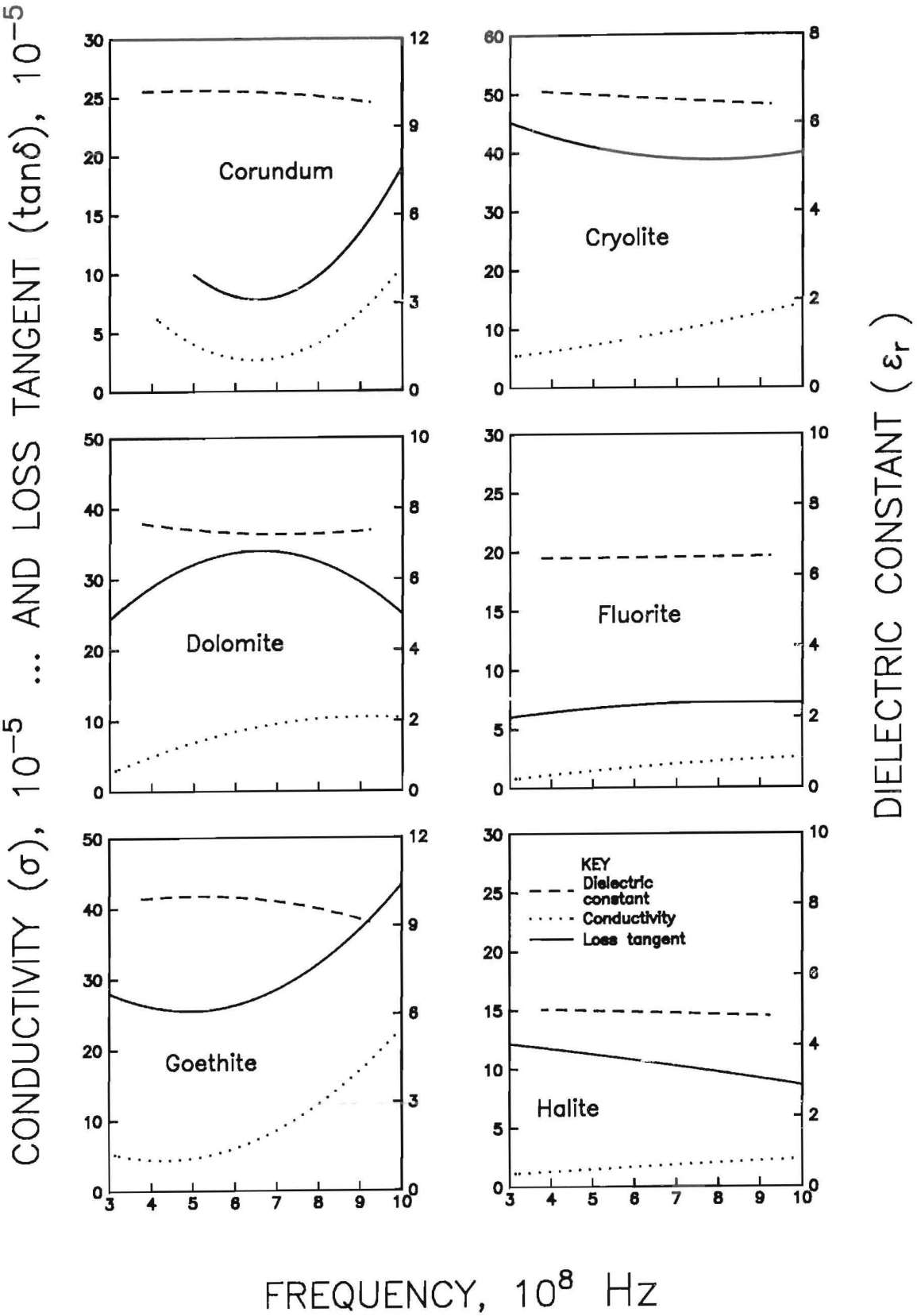
CONDUCTIVITY (σ), 10^{-5} ... AND LOSS TANGENT (tanδ), 10^{-5}
DIELECTRIC CONSTANT (ε_r)
FREQUENCY, 10^8 Hz
Corundum
Cryolite
Dolomite
Fluorite
Goethite
Halite
KEY
Dielectric constant
Conductivity
Loss tangent

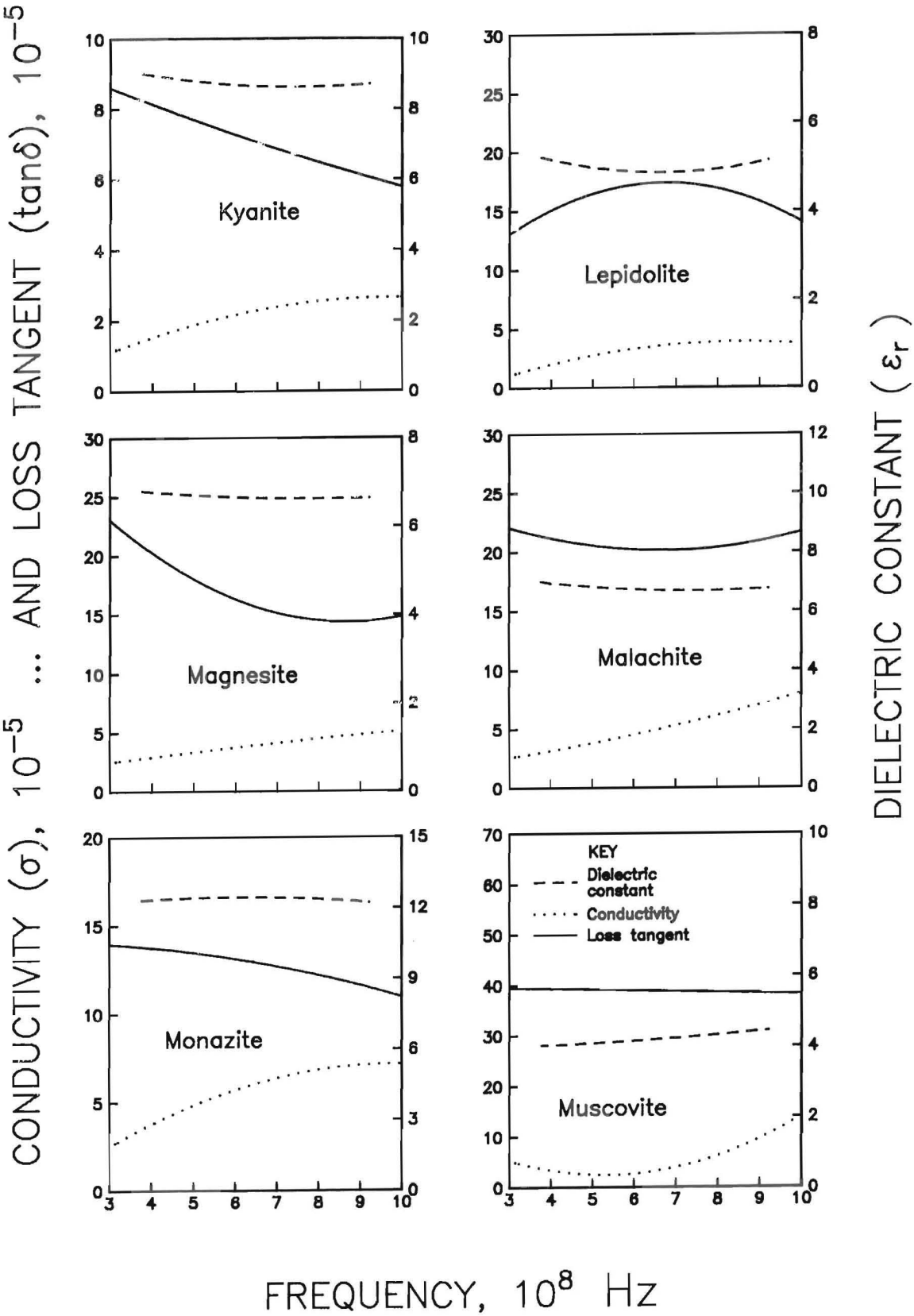
CONDUCTIVITY (σ), 10^{-5} ... AND LOSS TANGENT (tanδ), 10^{-5}
DIELECTRIC CONSTANT (ε_r)
Kyanite
Lepidolite
Magnesite
Malachite
Monazite
Muscovite
KEY
Dielectric constant
Conductivity
Loss tangent
FREQUENCY, 10^8 Hz

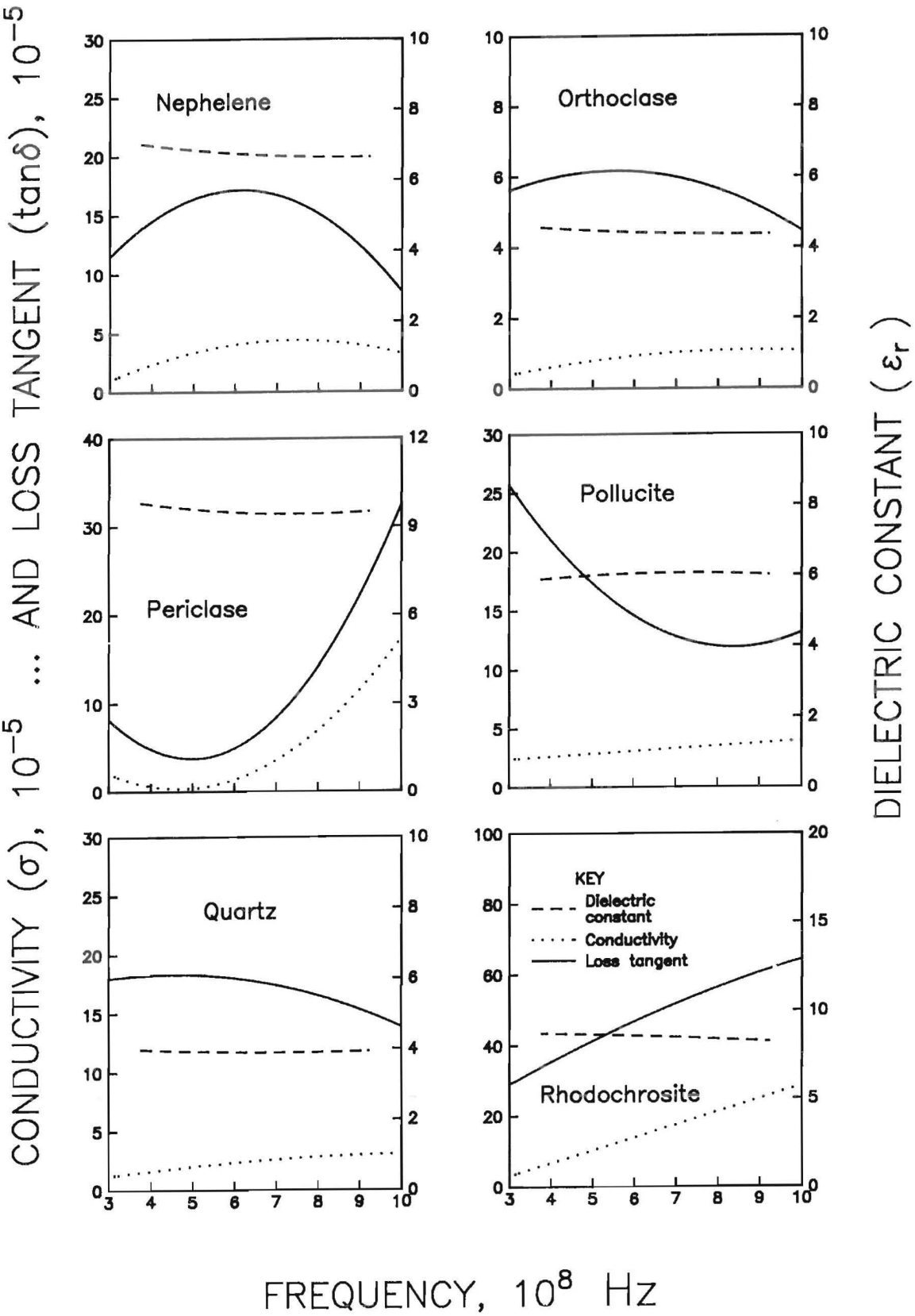
CONDUCTIVITY (σ), 10^{-5} ... AND LOSS TANGENT (tanδ), 10^{-5}
DIELECTRIC CONSTANT (ε_r)
Nephelene
Orthoclase
Periclase
Pollucite
Quartz
Rhodochrosite
KEY
Dielectric constant
Conductivity
Loss tangent
FREQUENCY, 10^8 Hz

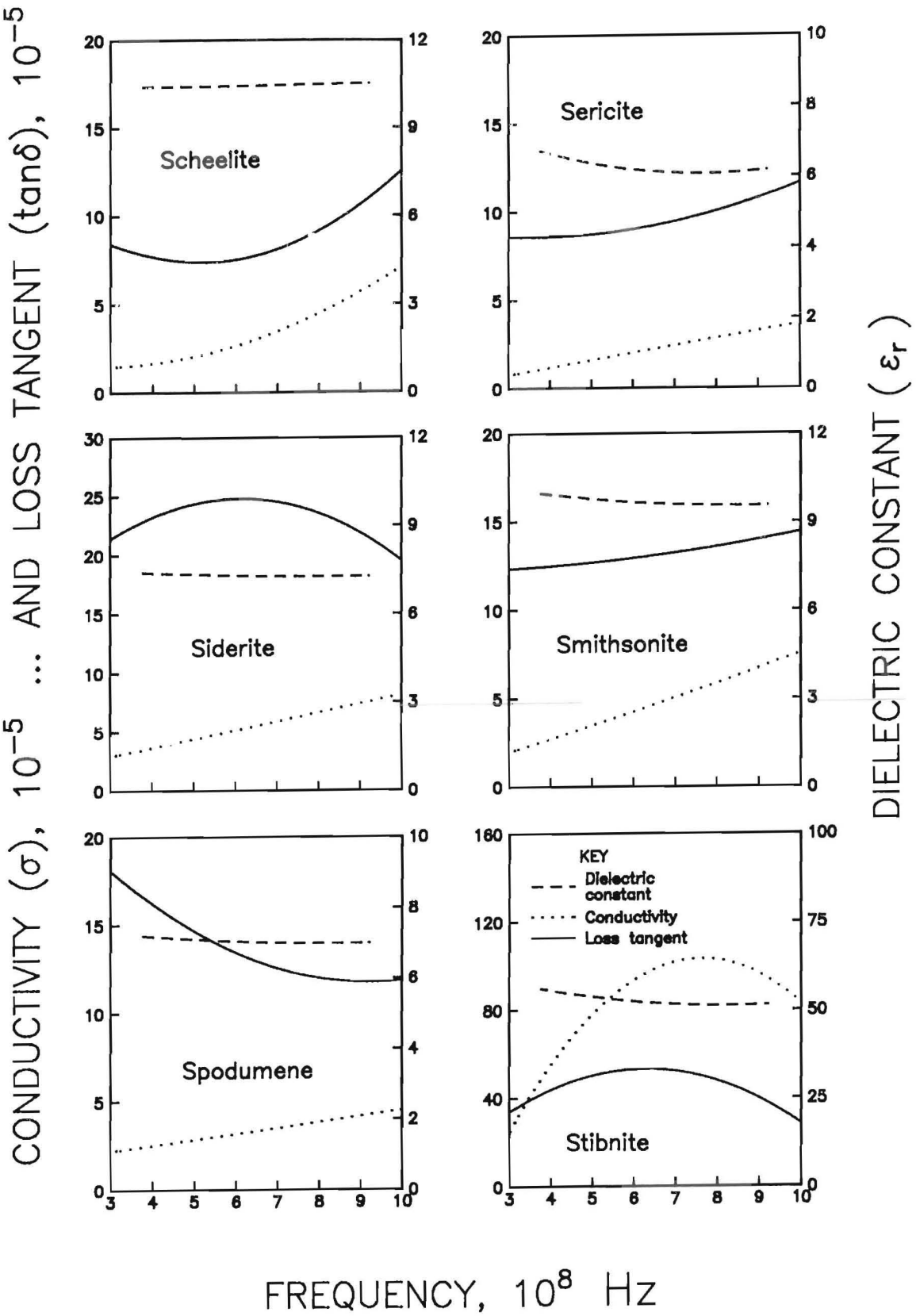
CONDUCTIVITY (σ), 10⁻⁵ ... AND LOSS TANGENT (tanδ), 10⁻⁵
DIELECTRIC CONSTANT (εr)
FREQUENCY, 10⁸ Hz
Scheelite
Sericite
Siderite
Smithsonite
Spodumene
Stibnite
KEY
Dielectric constant
Conductivity
Loss tangent

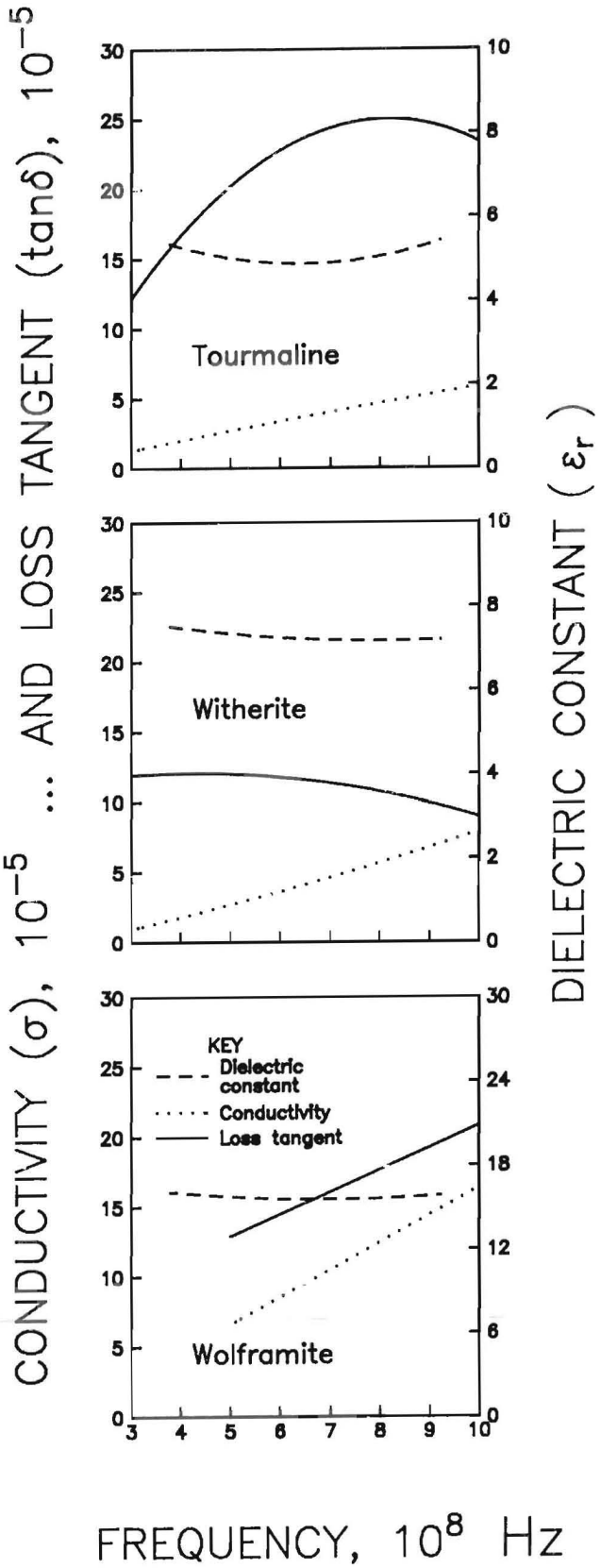
CONDUCTIVITY (σ), 10^{-5} ... AND LOSS TANGENT (tanδ), 10^{-5}
DIELECTRIC CONSTANT (ε_r)
Tourmaline
Witherite
Wolframite
KEY
Dielectric constant
Conductivity
Loss tangent
FREQUENCY, 10^8 Hz

APPENDIX B.–CHEMICAL COMPOSITION, LOCATION OF SAMPLE SOURCE, PURITY, AND ANALYSIS METHOD OF THE LOW-LOSS MINERALS MEASURED

Mineral name	*Chemical composition*	*Location of mineral source*	*Purity, pct*	*Impurities*	*Method of analysis*
Anhydrite	$CaSO_4$	Gabbs, Nye County, NV	98	Calcite	PET
Apatite	$(CaF)Ca_4(PO_4)_3$	Cerro de Mercado, Durango, Mexico.	100	None	PET
Aragonite	$CaCO_3$	ND	ND	ND	NA
Barite	$BaSO_4$	Socorro County, NM	100	None	PET
Bauxite	$Al_2O_3 \cdot 2H_2O$	Jamaica	ND	ND	NA
Beryl	$Be_3Al_2(SiO_3)_6$	Larimer County, CO	99	Albite, feldspar	PET
Biotite	$H_2K(Mg,Fe)_3Al(SiO_4)_3$	Arendal, Norway	98	Quartz, opaque, muscovite.	PET
Calcite	$CaCO_3$	Creel, Chilhuahua, Mexico	100	None	PET
Celestite	$SrSO_4$	San Luis Potosi, Mexico	100	None	PET
Cerussite	$PbCO_3$	ND	(1)	Trace: vaterite	XRD
Chromite	$FeCr_2O_4$	Mouat Mine, Nye, MT	99	Olivine	PET
Columbite	$(Fe,Mn)(Nb,Ta)_2O_6$	ND	98	Tantalite, cassiterite	PET
Corundum	Al_2O_3	ND	(1)	Trace: biaspore, possible trace: quartz, rutile	XRD
Cryolite	Na_3AlF_6	Ivigtut, Greenland	100	None	PET
Dolomite	$CaCO_3 \cdot MgCO_3$	ND	(1)	Trace-minor: quartz, possible trace: apatite, calcite.	XRD
Fluorite	CaF_2	Crystal Mountain, MT	99	Pyrite, quartz,chalcopyrite, magnetite, feldspar.	PET
Goethite	$Fe_2O_3 \cdot H_2O$	Rattlesnake Canyon, Socorro County, NM	99	Mica, quartz, silicates, calcite, pyrite,chalcopyrite.	PET
Halite	NaCl	ND	99.4	ND	CHEM
Kyanite	Al_2SiO_5	Ogilby, Imperial County, CA.	98	Quartz, limonite	PET
Lepidolite	$(OH,F)_2KLiAl_2Si_3O_{10}$	White Picacho District, Yavapai County, AZ.	99	Feldspar	PET
Magnesite	$MgCO_3$	Stevens County, WA.	100	None	PET
Malachite	$CuCO_3 \cdot Cu(OH)_2$	Cochise County, AZ	98	Quartz, limonite	PET
Monazite	$(Ce,La,Y,Th)Po_4$	ND	(1)	Possible trace: quartz	XRD
Muscovite	$H_2KAL_3(SiO_4)_3$	Lewiston, ID	98	ND	PET
Nephelene	$(Na,K)AlSiO_4$	Bancroft, Ontario, Canada	93	Muscovite, sodalite, analcite.	PET
Orthoclase	$KAlSi_3O_8$	ND	ND	ND	NAP
Periclase	MgO	ND	(1)	Possible trace: brucite, quartz, forsterite.	XRD
Pollucite	$H_2Cs_4Al_4(SiO_3)_9$	Karibib, Southwest Africa	93	Mica, quartz,feldspar, leidolite.	PET
Quartz	SiO_2	12 miles Southwest of Anaconda, MT.	100	None	PET
Rhodochrosite	$MnCO_3$	Mina Capillitas, Catamarca Province, Argentina.	99	Pyrite, limonite	PET
Scheelite	$CaWO_4$	Okanogan County, WI	99	Limonite, pyrite	PET
Sericite	$(H,K)AlSiO_4$	ND	ND	ND	NAP
Siderite	$FeCO_3$	Roxybury, CT.	100	None	PET
Smithsonite	$ZnCO_3$	Mauguarichic, Chihuahua, Mexico.	99	Sphalerite, limonite	PET
Spodumene	$LiAl(SiO_4)_3$	ND	(1)	Possible trace: quartz	XRD
Stibnite	$CaAl_2Si_7O_{18} \cdot 7H_2O$	ND	(1)	Possible trace: kermesite, valentinite, ankerite, gudmundite.	XRD
Tourmaline	$HgAl_3(B \cdot OH)_2Si_4O_{19}$	Belmont Mountains, Maricopa County, AZ.	98	Quartz, mica	PET
Witherite	$BaCO_3$	Settling Stones Mine, Northumberland, England.	98	Pyrite, chalcopyrite, sphalerite.	PET
Wolframite	$(Fe,Mn)WO_4$	Black Pearl Mine, Bagdad, Yavapai County, AZ.	99	Limonite, scheelite, quartz, pyrite, fluorite, biotite, muscovite.	PET

[1]Primary constituent.
NAP Not applicable.
ND Not determined.
CHEM Chemical.
PET Petrographic analysis.
XRD X-ray diffraction.

APPENDIX C.–ABBREVIATIONSAND SYMBOLS USED IN THIS REPORT

a	waveguide width	$\tan\delta$	loss tangent
b	waveguide height	u	constant
C	capacitance	X	reactance
C_o	constant of proportionality	X_{in}	input reactance
C_p	specific heat	X_o	characteristic reactance
c	speed of light	$\underline{X}$	distance along waveguide width
E	electric field strength	Z	impedance
E_o	magnitude of the electric field	Z_{in}	input impedance
E_p	peak electric field	Z_o	characteristic impedance
E_s	standing electric field	α	attenuation constant
E_t	traveling electric field	α_{dip}	dipole polarization
f	frequency	α_{el}	electron polarization
f_c	cutoff frequency	α_{int}	interfacial polarization
GPR	ground penetrating radar	α_{ion}	ionic polarization
ISM	industrial, scientific, medical	αp	total polarization
j	imaginary quantity, $\sqrt{-1}$	β	phase constant
k	constant of proportionality	Γ	reflection coefficient
ℓ	length of transmission line	Γ_{load}	load reflection coefficient
NBS	National Bureau of Standards	γ	propagation constant
P	power	ϵ	permittivity
P_a	applied power	ϵ''	dielectric loss factor
P_d	power density	ϵ_o	permittivity of free space
R	resistance	ϵ_r	dielectric constant or relative permittivity
R_c	constant		
R_{in}	input resistance	η_g	intrinsic impedance of waveguide
R_o	characteristic resistance	η_o	intrinsic impedance of free space
RF	radio frequency	λ_g	waveguide wavelength
T	temperature	λ_o	wavelength in free space
T_f	limiting temperature	ρ	density
T_o	ambient temperature	σ	electrical conductivity
t	time	ω	angular frequency

Note.–This list does not include the unit of measure abbreviations listed at the front of this report.

* U.S. GOVERNMENT PRINTING OFFICE: 611-012/00,003

INT.–BU. OF MINES, PGH.,PA. 28787